Efficiently solving the dynamics of many-body localized systems at strong disorder

Giuseppe De Tomasi, Frank Pollmann, Markus Heyl

Angaben zur Veröffentlichung / Publication details:

De Tomasi, Giuseppe, Frank Pollmann, and Markus Heyl. 2019. "Efficiently solving the dynamics of many-body localized systems at strong disorder." *Physical Review B* 99 (24): 241114(R). https://doi.org/10.1103/physrevb.99.241114.

Rapid Communications

Efficiently solving the dynamics of many-body localized systems at strong disorder

Giuseppe De Tomasi,[1,3] Frank Pollmann,[1,2] and Markus Heyl[3]

[1]*Department of Physics, T42, Technische Universität München, 85747 Garching, Germany*

[2]*Munich Center for Quantum Science and Technology (MCQST), Schellingstr. 4, D-80799 München, Germany*

[3]*Max-Planck-Institut für Physik Komplexer Systeme, Nöthnitzer Straße 38, 01187-Dresden, Germany*

(Received 23 October 2018; revised manuscript received 14 June 2019; published 28 June 2019)

We introduce a method to efficiently study the dynamical properties of many-body localized systems in the regime of strong disorder and weak interactions. Our method reproduces qualitatively and quantitatively the time evolution with a polynomial effort in system size and independent of the desired time scales. We use our method to study quantum information propagation, correlation functions, and temporal fluctuations in one- and two-dimensional many-body localization systems. Moreover, we outline strategies for a further systematic improvement of the accuracy and we point out relations of our method to recent attempts to simulate the time dynamics of quantum many-body systems in classical or artificial neural networks.

DOI: 10.1103/PhysRevB.99.241114

Introduction. Experiments in quantum simulators, such as ultracold atoms in optical lattices and trapped ions, have nowadays achieved access to the dynamical properties of closed quantum many-body systems far from equilibrium [1–4]. Therefore, it has become possible to experimentally study intrinsically dynamical phenomena that are challenging to realize and probe on other platforms. One prominent example constitutes the many-body localized phase in systems with strong disorder, whose signatures have been observed in a series of recent experiments [5–9]. Many-body localization (MBL) describes a nonergodic phase of matter, in which particles are localized due to the presence of a strong disorder potential [10–13], extending the phenomenon of Anderson localization [14] to the interacting case. Importantly, the presence of interactions makes the dynamical properties much richer [15–21]. In particular, interactions give rise to an additional dephasing mechanism, allowing entanglement and quantum information propagation even though particle and energy transport is absent [15–18,22]. Describing, however, quantitatively this interaction-induced propagation for large systems beyond exact numerical methods has remained as one of the main challenges.

In this work, we introduce an efficient numerical method to compute the dynamics of weakly interacting fermions in a fully localized MBL phase. The method is controlled by the interaction strength and we find that the error remains bounded in time over many temporal decades up to the asymptotic long-time dynamics of quantum information transport in MBL systems, which occurs on timescales exponentially in system size. The computational resources for computing local observables and correlation functions in our approach scale only polynomially in system size and are even independent of the targeted time in the dynamics. We utilize the method to study the dynamics of interacting fermions not only in one dimension (1D) but also in two dimensions (2D) for up to 200 lattice sites. After benchmarking our approach by comparing the characteristic entanglement entropy growth with exact diagonalization, we study the quantum information transport on the basis of the quantum Fisher information [7,23–28], the logarithmic light cone in correlation functions [22,29–36], and temporal fluctuations of observables, both for 1D and 2D. Finally, we point out a connection between our approach and recent ideas to encode quantum states into classical and artificial neural networks.

Models and methods. At sufficiently strong disorder the MBL eigenstates are expected to be adiabatically connected to the noninteracting ones [37,38]. In such a case the system is fully described by an extensive number of quasilocal integral of motions $\{\hat{I}_l\}$ [29,39–46], which emphasize an emerging weak form of integrability [37,41]. In this case the Hamiltonian of the system exhibits a representation of the following form:

$$\hat{H} = \sum_l J_l^{(1)} \hat{I}_l + \sum_{l,m} J_{l,m}^{(2)} \hat{I}_l \hat{I}_m + \cdots , \tag{1}$$

where l enumerates the sites of the underlying lattice. For the considered weakly interacting case, higher-order couplings between the integrals of motion $\hat{I}_l$ become exponentially suppressed in the interaction strength, so that we can terminate the expansion as done in Eq. (1). Moreover, it is expected that $J_{l,m}^{(2)} \sim e^{-d(l,m)/\xi}$ with $d(l,m)$ the spatial distance of the two involved lattice sites l and m and ξ denoting the localization length. While it is expected that this so-called l-bit representation exists, it has remained as a central challenge (i) to construct explicitly the integrals of motion $\{\hat{I}_l\}$ and (ii) to make use of the l-bit Hamiltonian to compute its dynamics.

In this work, we show that in the limit of weakly interacting fermions at strong disorder both of these challenges can be efficiently solved. In this limit we can decompose the Hamiltonian $\hat{H} = \hat{H}_0 + \hat{\mathcal{V}}$ with $\hat{H}_0$ a noninteracting Anderson-localized system and $\hat{\mathcal{V}}$ the interaction part, whose strength we denote by V. We take as the $\hat{I}_l$'s the integrals of motion of $\hat{H}_0 = \sum_l \epsilon_l \hat{I}_l$ with $\hat{I}_l = \hat{\eta}_l^\dagger \hat{\eta}_l$ and $\hat{\eta}_l^\dagger$ ($\hat{\eta}_l$) denoting the creation (annihilation) operator for a single-particle Anderson eigenstate ϕ_l with eigenvalue ϵ_l. As a second step, we express $\hat{\mathcal{V}} = \sum_{lmnk} \mathcal{B}_{lmnk} \hat{\eta}_l^\dagger \hat{\eta}_m \hat{\eta}_n^\dagger \hat{\eta}_k$ in terms of the $\{\hat{\eta}_l\}$. Then

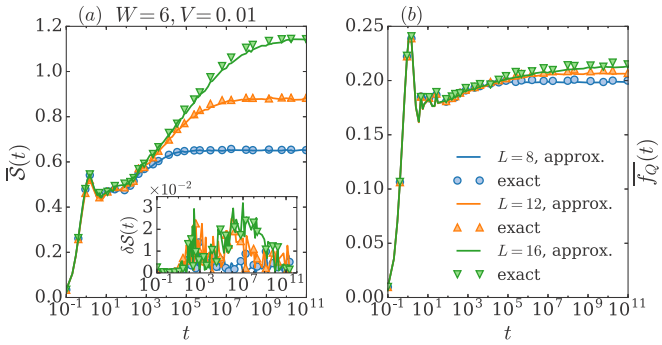

FIG. 1. (a) Bipartite half-chain entanglement entropy $\overline{S}(t)$ after a global quantum quench for several systems sizes (L) in 1D. $\overline{S}(t)$ has been calculated using the exact Hamiltonian $\hat{H}$ (exact) and the effective model $\hat{H}^{\text{eff}}$ (approx.). The inset shows the relative error $\delta\mathcal{S}(t) = |\overline{\mathcal{S}}(t) - \mathcal{S}^{\text{approx}}(t)|/\overline{\mathcal{S}}(t)$, between the entanglement entropy calculated with $\hat{H}$ and the one calculated with $\hat{H}^{\text{eff}}$. (b) QFI for the 1D MBL system for several system sizes compared with exact results.

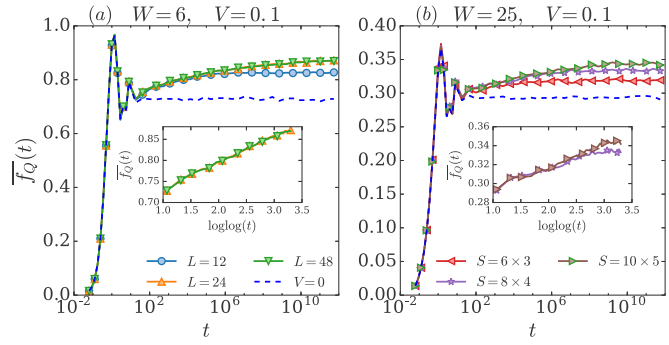

FIG. 2. (a) Disorder-averaged QFI density $[\overline{f_Q}(t) = \overline{\mathcal{F}_Q}(t)/2N]$ for the 1D MBL model for several system sizes (L) and a fixed disorder and interaction strength. The inset shows $\overline{f_Q}(t)$ in a suitable scale to underline that $\overline{f_Q}(t) \sim \log\log t$. (b) Disorder-averaged QFI density $[\overline{f_Q}(t)]$ for the 2D model for several system sizes (S) and a fixed disorder and interaction strength. The inset shows that also in this case $\overline{f_Q}(t) \sim \ln\ln t$. For both panels the evolution has been obtained using $\hat{H}^{\text{eff}}$. Dashed lines are for the noninteracting case ($V = 0$) for the largest system size in each panel.

we neglect all contributions that do not commute with the $\{\hat{I}_l\}$ so that we arrive at the following desired l-bit Hamiltonian:

$$\hat{H}^{\text{eff}} = \sum_l \epsilon_l \hat{\eta}_l^\dagger \hat{\eta}_l + \sum_{l,m} \mathcal{B}_{l,m} \hat{\eta}_l^\dagger \hat{\eta}_l \hat{\eta}_m^\dagger \hat{\eta}_m, \tag{2}$$

with $\mathcal{B}_{l,m} = \mathcal{B}_{llmm} - \mathcal{B}_{lmlm}$. This construction relies on the perturbative nature of an MBL phase, in which the integrals of motion of the system $\{\hat{I}_l\}$ can be obtained perturbatively from the noninteracting ones $\{\hat{\eta}_l^\dagger \hat{\eta}_l\}$ [10,29,40,44,46]. Thus, as a first approximation in the limit of weak interactions, the integrals of motion can be taken as those of the noninteracting case. In the concluding discussion we will outline how one can improve systematically the accuracy of the l bits by accounting for higher orders in V [47]. For the following, we will use the representation above and show that it is already sufficient to capture quantitatively the dynamics for small V.

Having discussed the construction of the l-bit Hamiltonian, we now outline how this can be used to study dynamics, which is based on two main properties. First, the time evolution of $\hat{\eta}_l$ and $\hat{\eta}_l^\dagger$ can be determined analytically via $\hat{\eta}_l^\dagger(t) = \exp[it\epsilon_l + it\sum_m \tilde{\mathcal{B}}_{l,m}\hat{\eta}_m^\dagger\hat{\eta}_m]\hat{\eta}_l^\dagger$ where $\tilde{\mathcal{B}}_{l,m} = \mathcal{B}_{m,l} + \mathcal{B}_{l,m}$.

Second, for an initial state $|\psi\rangle$, which is a product state in terms of the bare fermions, i.e., Gaussian, the expectation values of time-evolved local observables and correlation functions can be reduced to the evaluation of Slater determinants, which can be done very efficiently. For example, for a generic local observable $\hat{A} = \sum_{l,m} a_{l,m}\hat{\eta}_l^\dagger\hat{\eta}_m$, we need only to calculate $\langle\hat{\eta}_l^\dagger\hat{\eta}_m(t)\rangle = e^{it(\epsilon_l-\epsilon_m)}\langle\hat{\eta}_l^\dagger e^{it\sum_p(\tilde{\mathcal{B}}_{l,p}-\tilde{\mathcal{B}}_{p,m})\hat{\eta}_p^\dagger\hat{\eta}_p}\hat{\eta}_m\rangle$, where $\langle\cdots\rangle = \langle\psi|\cdots|\psi\rangle$. The term $\langle\hat{\eta}_l^\dagger e^{it\sum_p(\tilde{\mathcal{B}}_{l,p}-\tilde{\mathcal{B}}_{p,m})\hat{\eta}_p^\dagger\hat{\eta}_p}\hat{\eta}_m\rangle$ can be efficiently computed using Wick's theorem [48], interpreting $e^{it\sum_p(\tilde{\mathcal{B}}_{l,p}-\tilde{\mathcal{B}}_{m,p})\hat{\eta}_p^\dagger\hat{\eta}_p}$ as an effective time-evolution operator of the quadratic Hamiltonian $\hat{H}^{(l,m)} = \sum_p(\tilde{\mathcal{B}}_{l,p} - \tilde{\mathcal{B}}_{m,p})\hat{\eta}_p^\dagger\hat{\eta}_p$. Importantly, such initial conditions are typical choices in theory [15,16,20,21,49–52] and have been realized in the MBL context experimentally [5,6,8,9].

For concreteness, we demonstrate our method for the Hamiltonian [16,53–56]

$$\hat{H} := -\frac{1}{2}\sum_{\langle\mathbf{i},\mathbf{j}\rangle}(\hat{c}_\mathbf{i}^\dagger\hat{c}_\mathbf{j} + \text{H.c.}) + \sum_\mathbf{j} h_\mathbf{j}\hat{n}_\mathbf{j} + V\sum_{\langle\mathbf{i},\mathbf{j}\rangle}\hat{n}_\mathbf{i}\hat{n}_\mathbf{j}, \tag{3}$$

where $\hat{c}_\mathbf{j}^\dagger$ ($\hat{c}_\mathbf{j}$) is the fermionic creation (annihilation) operator at site $\mathbf{j}$ and $\hat{n}_\mathbf{j} = \hat{c}_\mathbf{j}^\dagger\hat{c}_\mathbf{j}$. $\{h_\mathbf{j}\}$ are random fields uniformly distributed between $[-W, W]$, and V is the interaction strength. We study the system both in a 1D lattice of size L with periodic boundary conditions and defined in a rectangular lattice (2D) of size $S = L \times \frac{L}{2}$ with periodic and open boundary conditions respectively in the x and in the y direction. We focus on half-filling $N/L = 1/2$ ($N/|S| = 1/2$) with N the number of fermions. The 1D system is believed to have an MBL phase at strong disorder [54–59]. The 2D case, on the other hand, has largely remained elusive due to the lack of efficient methods to simulate sufficiently large system sizes. A recent experiment has given evidence of an MBL phase in a bosonic 2D system [6]. Nevertheless, it is currently under debate whether MBL can be stable at all in 2D [6,8,60–64]. The proposed mechanism for the breakdown of MBL relies on rare resonances which, however, only manifest on very long time-scales, below which our l-bit description, Eq. (2) could still be accurate at intermediate timescales.

Following our prescription outlined before, we first diagonalize the noninteracting model by introducing $\hat{\eta}_l^\dagger = \sum_\mathbf{i}\phi_l(\mathbf{i})\hat{c}_\mathbf{i}^\dagger$. This then leads to $\mathcal{B}_{l,m} = V\sum_{\langle\mathbf{i},\mathbf{j}\rangle}[|\phi_l(\mathbf{i})|^2|\phi_m(\mathbf{j})|^2 - \phi_l(\mathbf{i})\phi_m(\mathbf{i})\phi_l(\mathbf{j})\phi_m(\mathbf{j})]$. In the remainder, we choose staggered initial states of charge-density type both for 1D $|\psi\rangle = \prod_{s=-L/4}^{L/4-2} c_{2s}^\dagger|0\rangle$ and for 2D $|\psi\rangle = \prod_{y=-L/2}^{L/2-1}\prod_{x=-L/4}^{L/4-2} c_{(2x,y)}^\dagger|0\rangle$, motivated by recent experiments [6]. Disorder-averaged quantities will be indicated with an overline, e.g., $\overline{\langle\hat{n}_\mathbf{i}\rangle}$.

Benchmark for quantum-information propagation. We now compare the exact dynamics of $\hat{H}$ with that generated by $\hat{H}^{\text{eff}}$. For the benchmark we choose to study quantum-information

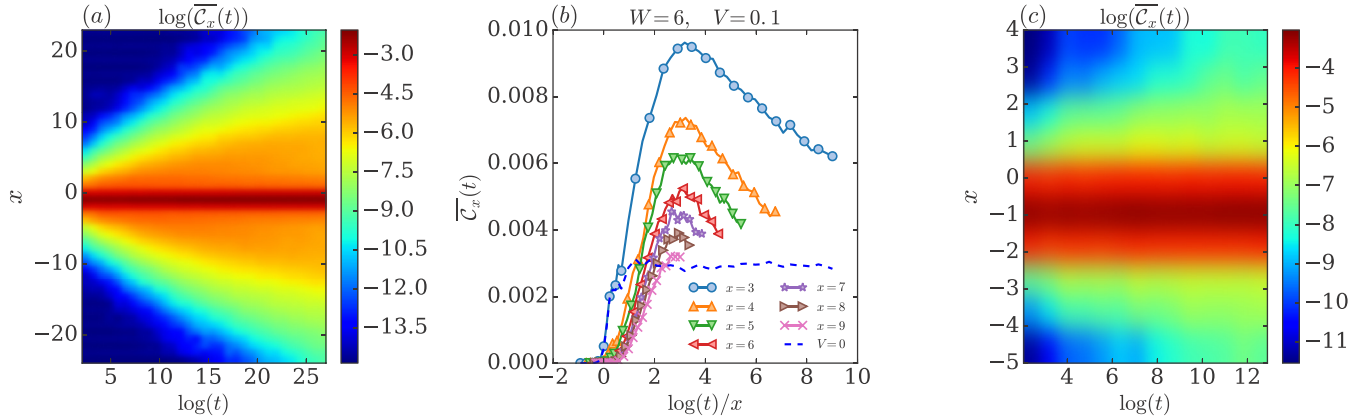

FIG. 3. (a) Logarithmic light-cone calculated using the $\mathcal{C}_x(t)$ for the effective model in 1D. (b) $\mathcal{C}_x(t)$ as a function of time; the time has been properly rescaled to get the collapse of the curves. It also shows the noninteracting case ($V = 0$) (dashed line). For both panels (a) and (b) $L = 48$. (c) Logarithmic light cone for the 2D case with $S = 10 \times 5$ in the x direction calculated using $\mathcal{C}_{x,0}(t)$ evolved with the effective model with $W = 25$ and $V = 0.1$.

(entanglement) propagation, which inherits one of the central and nontrivial features of MBL phases. In Fig. 1 we show data for two measures, both obtained using exact diagonalization and via our effective Hamiltonian [65]. First, this includes the half-chain entanglement entropy

$$\mathcal{S}(t) = -\mathrm{Tr}\hat{\rho}_{L/2}(t)\log\hat{\rho}_{L/2}(t), \tag{4}$$

where $\hat{\rho}_{L/2}(t)$ denotes the reduced density matrix of half of the system. Second, we study the quantum Fisher information (QFI) related to the initial charge-density pattern defined by

$$\mathcal{F}_Q(t) = 4[\langle\hat{\mathcal{O}}(t)^2\rangle - \langle\hat{\mathcal{O}}(t)\rangle^2], \quad \hat{\mathcal{O}} = \sum_x (-1)^x \hat{n}_x. \tag{5}$$

The QFI probes the propagation of quantum correlations and is an entanglement witness [7,23–28], that has been also measured experimentally in the MBL context [7].

As we can see from Fig. 1(a) the effective model reproduces not only qualitatively the unbounded logarithmic growth of the entanglement entropy [15,42], but even more importantly also quantitatively correctly in the long-time limit. In particular, the inset in Fig. 1(a) shows that the relative error $\delta\mathcal{S}(t) = |\mathcal{S}(t) - \mathcal{S}^{\mathrm{approx}}(t)|/\mathcal{S}(t)$ is a bounded function of time and remains smaller than 3% for all times. Let us note that the results for $\delta\mathcal{S}(t)$ gives evidence that our method not only reproduces the logarithmic growth after disorder averaging but even for individual random configurations. Similarly, also for the QFI the dynamics generated by the effective Hamiltonian follows closely the exact one [see Fig. 1(b) where we define the QFI density $f_Q = \mathcal{F}_Q/2N$ [7]]. While the entanglement entropy serves as a prime example for MBL properties, its computation within our method is not scalable to large system sizes. This, however, is different for the QFI which can still be computed efficiently even for large systems, which allows us to also access it in 2D (see below). It is important to note that our method reproduces the exact dynamics also for times longer than the naively expected range of validity of perturbation theory ($\sim 1/V$), which can be understood from a statistical analysis of the discarded elements $\mathcal{B}_{l,m,n,k}$ [66].

Results. Having shown that our method reproduces quantitatively the exact dynamics at a controlled error, we now aim to further demonstrate the capabilities of our method. We target this goal by addressing several aspects of MBL systems which up to now have not been accessible or could not be settled due to system size limitations. This includes aspects of quantum-information propagation, logarithmic spread of correlations, and temporal fluctuations of local observables both in 1D and 2D. In the following, we choose a larger interaction strength $V = 0.1$ instead of $V = 0.01$ as used for Fig. 1, which increases slightly the relative error in the computed quantities, but at the same time allows us to amplify the influence of interaction effects.

Figure 2 shows $f_Q(t)$ for the 1D case (a) and the 2D case (b), respectively, now computed for much larger systems than done for the benchmark in Fig. 1. For the 2D model we choose the QFI along the x direction, i.e., $\hat{\mathcal{O}} = \sum_x (-1)^x \hat{n}_x$ with $\hat{n}_x := \hat{n}_{(x,0)}$. For comparison we also include the results for the noninteracting models, which show quick saturation to a system-size-independent value. For nonvanishing interactions, the behavior of $\overline{\mathcal{F}_Q}(t)$ changes completely and we observe a slow growth, which is consistent with $\overline{\mathcal{F}_Q}(t) \sim \log\log t$ (insets) over many decades in time and almost independent of system size. As a consequence, we are capable of demonstrating slow quantum-information propagation in 2D MBL systems, which up to now has not been possible by other methods [29,60–62]. In a recent experiment in trapped ions implementing a long-range disordered Ising model evidence for an intermediate $\overline{\mathcal{F}_Q}(t) \sim \log t$ growth has been found [7], which, however, might be due to the fact that the system could be in an algebraic MBL phase [67,68], leading to $\mathcal{B}_{0,l} \sim 1/l^\beta$ with power law instead of exponential dependence [67–70].

As a next step we aim at studying quantum correlation spreading via the two-point connected correlation function, defined by

$$\mathcal{C}_x(t) = |\langle\hat{n}_x(t)\hat{n}_0(t)\rangle - \langle\hat{n}_x(t)\rangle\langle\hat{n}_0(t)\rangle|. \tag{6}$$

$\mathcal{C}_x(t)$ has been used in several quantum systems [31–36] to quantify the time t required to correlate two sites at some

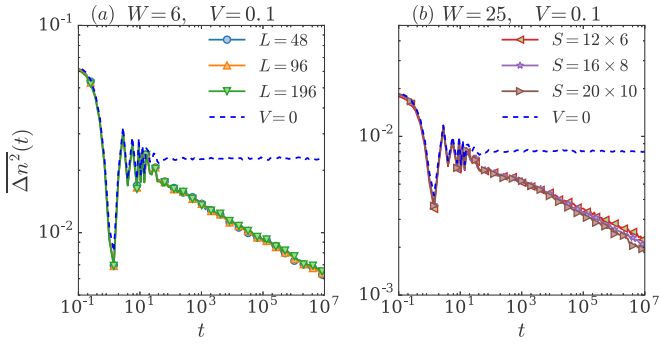

FIG. 4. (a) Disorder-averaged time fluctuations $[\overline{\Delta n^2}(t)]$ for several system sizes L for the 1D case, $\overline{\Delta n^2}(t) \sim t^{-\alpha}$. (b) $\overline{\Delta n^2}(t)$ for several system sizes S for the 2D case; also in this case its decay is consistent with an algebraic decay in time. The noninteracting case ($V = 0$) is also shown (dashed lines) for the largest system size. For both cases the evolution has been performed using $\hat{H}^{\text{eff}}$.

distance x, giving rise to the so-called light cone of propagation of correlations. Moreover, $\mathcal{C}_x(t)$ has been measured in a recent experiment in a disordered Bose-Hubbard chain to probe the existence of an MBL phase [30]. The 1D case we address in Fig. 3(a), where we show a color plot of $\mathcal{C}_x(t)$ displaying the logarithmic light cone [30–36,71,72] over many decades with quantum correlations spreading in space only logarithmically slowly in time. Interestingly, however, we find that there exists a timescale $t_x^\star$ beyond which $\mathcal{C}_x(t)$ starts to decrease again [see Fig. 3(b)]. Remarkably, this indicates that quantum correlations are eventually scrambled in the long-time limit also in an MBL system, which might be consistent and even necessary with the expectation to reach in the long-time limit a state with volume-law entanglement entropy [73]. From the rescaling of the time axis used in Fig. 3(b) we find evidence that this correlation time $t_x^\star$ scales exponentially with the distance x ($\log t_x^\star \sim x$). In the case of an Anderson insulator ($V = 0$) quantum correlations are frozen in the long-time limit [15,42], implying the saturation to nonzero value of $\mathcal{C}_x(t)$ [Fig. 3(b), dashed line]. Finally, in Fig. 3(c) we study correlation spreading in 2D, where we found again, like in 1D, the same logarithmically slow propagation.

As opposed to an Anderson insulator it has been argued that an MBL system can show relaxation [59,74], meaning that expectation values of local observables reach at long time a stationary nonthermal value in the thermodynamic limit with decaying temporal fluctuations. Here, we use our method to reexamine the temporal fluctuations in 1D and to study them also for 2D systems. These are defined for $\hat{n}_x$ via

$$\Delta n^2(t) = \frac{1}{L}\sum_x \Delta n_x^2(t), \quad \Delta n_x^2(t) = (\langle \hat{n}_x\rangle(t) - \langle \hat{n}_x\rangle_{\text{tav}})^2, \tag{7}$$

where $\langle \hat{n}_x\rangle_{\text{tav}}$ denotes the long-time average of $\langle \hat{n}_x\rangle(t)$. As shown in Fig. 4, both in 1D and 2D the temporal fluctuations exhibit an algebraic decay with time, $\overline{\Delta n^2}(t) \sim t^{-\alpha}$. As a reference we have included also the data for the noninteracting cases ($V = 0$, dashed lines), where temporal fluctuations remain nonvanishing for all times. We find that the exponent α is proportional to the single-particle localization length ξ_{loc} [75], for which we now aim to give an analytical argument. This shows that our method not only can be used for numerically computing quantities but also for analytical predictions. For that purpose we consider a special initial state $|\psi\rangle = \prod_l^L \frac{\hat{\eta}_l + \hat{\eta}_l^\dagger}{\sqrt{2}}|0\rangle$ for which the calculations are simplified but which gives qualitatively the same decay of the temporal fluctuations [76]. For this state we find $\Delta n_x^2(t) = [\sum_{l\neq m}\phi_l(x)\phi_m(x)e^{i(\epsilon_l-\epsilon_m)t}\mathcal{Q}_{lm}]^2$ with $\mathcal{Q}_{lm} = 2^{-2}\prod_{k=l+1}^m \sin(A_k^{l,m}t)\prod_{s\neq k}\cos(A_s^{l,m}t)$ and $A_k^{l,m} = (V/2)(\tilde{\mathcal{B}}_{m,k} - \tilde{\mathcal{B}}_{l,k}) \sim Ve^{-[\min(|m-k|,|l-k|)/\xi_{\text{loc}}]}$. The sum over (l, m) can be restricted only to eigenstates, whose centers are located within a distance ξ_{loc} away from x. Each term of the cos's and sin's with argument $A_k^{l,m}$ decays exponentially in k, which leads to a power-law in time [51] with an exponent proportional to ξ_{loc}, implying $\Delta n_x^2(t) \sim t^{-c\xi_{\text{loc}}}$ [20].

Conclusions. In this work, we have formulated a method which allows one to efficiently study the dynamics of weakly interacting localized fermions. The accuracy of the approach can be further increased systematically by taking into account those contributions to the interaction term, which are not commuting with the bare integrals of motion $\hat{I}_l$ and which have been completely neglected in the present study. For example, to lowest order they can be accounted using a Schrieffer-Wolff transformation. Our method can be applied to any weakly interacting MBL system, which exhibits an l-bit representation, not only limited to the quantum quench dynamics studied here. Thus, it can be used also to study, for example, driven Floquet MBL systems [77] such as they appear in discrete time crystals [78,79], MBL bosonic systems, algebraic MBL [67–69] and MBL weakly coupled with thermal baths [80–83]. However, let us note that even in cases where an MBL phase might not be stable asymptotically for infinite system sizes and infinite times, our method might still provide a description on intermediate timescales (e.g., MBL in 2D [6,8,60–64]).

Overall, our method maps the dynamical quantum many-body problem onto a system of classical degrees of freedom of mutually commuting operators, similar in spirit to recent works where dynamical problems have been solved using classical [84] or artificial neural networks [85]. Instead of solving the problem in the basis of the bare particles, our work shows that a simple basis transformation onto more convenient degrees of freedom can improve the accuracy and efficiency dramatically, which might also be of relevance for the aforementioned approaches.

Note added. Very recently, the dynamics of one-point functions has been computed using a self-consistent Hartree-Fock method, which scales polynomially in system size and time [86].

Acknowledgments. We thank J. H. Bardarson, S. Bera, A. Burin, A. Eckardt, I. M. Khaymovich, M. Knap, and D. Trapin for several illuminating discussions. F.P. acknowledges the support of the DFG Research Unit FOR 1807 through Grant No. PO 1370/2-1, TRR80, the Nanosystems Initiative Munich (NIM) by the German Excellence Initiative, and the European Research Council (ERC) under the European Union's Horizon 2020 Research and Innovation Program (Grant Agreement

No. 771537). This research was conducted in part at the KITP, which is supported by NSF Grant No. NSF PHY-1748958. M.H. acknowledges support from the Deutsche Forschungsgemeinschaft via the Gottfried Wilhelm Leibniz Prize program. F.P. acknowledges support from the DFG under Germanys Excellence Strategy - EXC-2111-390814868

[1] I. Bloch, J. Dalibard, and W. Zwerger, Rev. Mod. Phys. **80**, 885 (2008).
[2] R. Blatt and C. F. Roos, Nat. Phys. **8**, 277 (2012).
[3] I. Bloch, J. Dalibard, and S. Nascimbène, Nat. Phys. **8**, 267 (2012).
[4] I. M. Georgescu, S. Ashhab, and F. Nori, Rev. Mod. Phys. **86**, 153 (2014).
[5] M. Schreiber, S. S. Hodgman, P. Bordia, H. P. Lüschen, M. H. Fischer, R. Vosk, E. Altman, U. Schneider, and I. Bloch, Science **349**, 842 (2015).
[6] J.-y. Choi, S. Hild, J. Zeiher, P. Schauß, A. Rubio-Abadal, T. Yefsah, V. Khemani, D. A. Huse, I. Bloch, and C. Gross, Science **352**, 1547 (2016).
[7] J. Smith, A. Lee, P. Richerme, B. Neyenhuis, P. W. Hess, P. Hauke, M. Heyl, D. A. Huse, and C. Monroe, Nat. Phys. **12**, 907 (2016).
[8] P. Bordia, H. P. Lüschen, S. S. Hodgman, M. Schreiber, I. Bloch, and U. Schneider, Phys. Rev. Lett. **116**, 140401 (2016).
[9] H. P. Lüschen, P. Bordia, S. Scherg, F. Alet, E. Altman, U. Schneider, and I. Bloch, Phys. Rev. Lett. **119**, 260401 (2017).
[10] D. Basko, I. Aleiner, and B. Altshuler, Ann. Phys. (NY) **321**, 1126 (2006).
[11] R. Nandkishore and D. A. Huse, Annu. Rev. Condens. Matter Phys. **6**, 15 (2015).
[12] D. A. Abanin, E. Altman, I. Bloch, and M. Serbyn, Rev. Mod. Phys. **91**, 021001 (2019).
[13] F. Alet and N. Laflorencie, C. R. Phys. **19**, 498 (2018).
[14] P. W. Anderson, Phys. Rev. **109**, 1492 (1958).
[15] J. H. Bardarson, F. Pollmann, and J. E. Moore, Phys. Rev. Lett. **109**, 017202 (2012).
[16] M. Žnidarič, T. Prosen, and P. Prelovšek, Phys. Rev. B **77**, 064426 (2008).
[17] M. Serbyn, Z. Papić, and D. A. Abanin, Phys. Rev. Lett. **110**, 260601 (2013).
[18] M. Žnidarič, Phys. Rev. B **97**, 214202 (2018).
[19] E. Canovi, D. Rossini, R. Fazio, G. E. Santoro, and A. Silva, Phys. Rev. B **83**, 094431 (2011).
[20] M. Serbyn, Z. Papić, and D. A. Abanin, Phys. Rev. B **90**, 174302 (2014).
[21] R. Singh, J. H. Bardarson, and F. Pollmann, New J. Phys. **18**, 023046 (2016).
[22] M. C. Bañuls, N. Y. Yao, S. Choi, M. D. Lukin, and J. I. Cirac, Phys. Rev. B **96**, 174201 (2017).
[23] S. L. Braunstein and C. M. Caves, Phys. Rev. Lett. **72**, 3439 (1994).
[24] P. Hauke, M. Heyl, L. Tagliacozzo, and P. Zoller, Nat. Phys. **12**, 778 (2016).
[25] D. Petz and C. Ghinea, *Quantum Probability and Related Topics* (World Scientific, Singapore, 2011), pp. 261–281.
[26] H. Strobel, W. Muessel, D. Linnemann, T. Zibold, D. B. Hume, L. Pezzè, A. Smerzi, and M. K. Oberthaler, Science **345**, 424 (2014).
[27] G. Tóth, Phys. Rev. A **85**, 022322 (2012).
[28] P. Hyllus, W. Laskowski, R. Krischek, C. Schwemmer, W. Wieczorek, H. Weinfurter, L. Pezzé, and A. Smerzi, Phys. Rev. A **85**, 022321 (2012).
[29] S. J. Thomson and M. Schiró, Phys. Rev. B **97**, 060201(R) (2018).
[30] A. Lukin, M. Rispoli, R. Schittko, M. E. Tai, A. M. Kaufman, S. Choi, V. Khemani, J. Léonard, and M. Greiner, Science **364**, 256 (2019).
[31] M. Cheneau, P. Barmettler, D. Poletti, M. Endres, P. Schauß, T. Fukuhara, C. Gross, I. Bloch, C. Kollath, and S. Kuhr, Nature (London) **481**, 484 (2012).
[32] G. Carleo, F. Becca, L. Sanchez-Palencia, S. Sorella, and M. Fabrizio, Phys. Rev. A **89**, 031602(R) (2014).
[33] A. M. Läuchli and C. Kollath, J. Stat. Mech.: Theory Exp. (2008) P05018.
[34] K. Najafi, M. A. Rajabpour, and J. Viti, Phys. Rev. B **97**, 205103 (2018).
[35] L. Bonnes, F. H. L. Essler, and A. M. Läuchli, Phys. Rev. Lett. **113**, 187203 (2014).
[36] L. Barbiero and L. Dell'Anna, Phys. Rev. B **96**, 064303 (2017).
[37] J. Z. Imbrie, J. Stat. Phys. **163**, 998 (2016).
[38] B. Bauer and C. Nayak, J. Stat. Mech.: Theory Exp. (2013) P09005.
[39] A. Chandran, I. H. Kim, G. Vidal, and D. A. Abanin, Phys. Rev. B **91**, 085425 (2015).
[40] V. Ros, M. Muller, and A. Scardicchio, Nucl. Phys. B **891**, 420 (2015).
[41] D. A. Huse, R. Nandkishore, and V. Oganesyan, Phys. Rev. B **90**, 174202 (2014).
[42] M. Serbyn, Z. Papić, and D. A. Abanin, Phys. Rev. Lett. **111**, 127201 (2013).
[43] N. Pancotti, M. Knap, D. A. Huse, J. I. Cirac, and M. C. Bañuls, Phys. Rev. B **97**, 094206 (2018).
[44] L. Rademaker, M. Ortuño, and A. M. Somoza, Ann. Phys. (NY) **529**, 1600322.
[45] M. H. Fischer, M. Maksymenko, and E. Altman, Phys. Rev. Lett. **116**, 160401 (2016).
[46] L. Rademaker, M. Ortuno, and A. M. Somoza, arXiv:1610.06238.
[47] See Supplemental Material at http://link.aps.org/supplemental/10.1103/PhysRevB.99.241114 for a statistical analysis of the discarded elements $\mathcal{B}_{l,m,n,k}$.
[48] M. E. Peskin and D. V. Schroeder, *An Introduction to Quantum Field Theory* (Addison-Wesley, Reading, MA, 1995).
[49] F. Iemini, A. Russomanno, D. Rossini, A. Scardicchio, and R. Fazio, Phys. Rev. B **94**, 214206 (2016).
[50] R. Vasseur, S. A. Parameswaran, and J. E. Moore, Phys. Rev. B **91**, 140202(R) (2015).
[51] S. Vardhan, G. De Tomasi, M. Heyl, E. J. Heller, and F. Pollmann, Phys. Rev. Lett. **119**, 016802 (2017).

[52] E. V. H. Doggen, F. Schindler, K. S. Tikhonov, A. D. Mirlin, T. Neupert, D. G. Polyakov, and I. V. Gornyi, Phys. Rev. B **98**, 174202 (2018).
[53] S. Bera, G. De Tomasi, F. Weiner, and F. Evers, Phys. Rev. Lett. **118**, 196801 (2017).
[54] D. J. Luitz, N. Laflorencie, and F. Alet, Phys. Rev. B **91**, 081103(R) (2015).
[55] A. Pal and D. A. Huse, Phys. Rev. B **82**, 174411 (2010).
[56] S. Bera, H. Schomerus, F. Heidrich-Meisner, and J. H. Bardarson, Phys. Rev. Lett. **115**, 046603 (2015).
[57] G. De Tomasi, S. Bera, J. H. Bardarson, and F. Pollmann, Phys. Rev. Lett. **118**, 016804 (2017).
[58] S. Bera and A. Lakshminarayan, Phys. Rev. B **93**, 134204 (2016).
[59] M. Serbyn, Z. Papić, and D. A. Abanin, Phys. Rev. X **5**, 041047 (2015).
[60] H. Théveniaut, Z. Lan, and F. Alet, arXiv:1902.04091.
[61] D. M. Kennes, Nat. Phys. **15**, 164 (2019).
[62] T. B. Wahl, A. Pal, and S. H. Simon, arXiv:1711.02678.
[63] W. De Roeck and J. Z. Imbrie, Philos. Trans. R. Soc., A **375**, 20160422 (2017).
[64] I.-D. Potirniche, S. Banerjee, and E. Altman, Phys. Rev. B **99**, 205149 (2019).
[65] See Supplemental Material at http://link.aps.org/supplemental/10.1103/PhysRevB.99.241114 for additional comparing data.
[66] See Supplemental Material at http://link.aps.org/supplemental/10.1103/PhysRevB.99.241114 for a statistical analysis of the discarded off-diagonal elements $\mathcal{B}_{l,m,n,k}$.
[67] G. De Tomasi, Phys. Rev. B **99**, 054204 (2019).
[68] T. Botzung, D. Vodola, P. Naldesi, M. Müller, E. Ercolessi, and G. Pupillo, arXiv:1810.09779.
[69] A. Safavi-Naini, M. L. Wall, O. L. Acevedo, A. M. Rey, and R. M. Nandkishore, Phys. Rev. A **99**, 033610 (2019).
[70] A. O. Maksymov and A. L. Burin, arXiv:1905.02286.
[71] D.-L. Deng, X. Li, J. H. Pixley, Y.-L. Wu, and S. Das Sarma, Phys. Rev. B **95**, 024202 (2017).
[72] S. Sahu, S. Xu, and B. Swingle, arXiv:1807.06086.
[73] See Supplemental Material at http://link.aps.org/supplemental/10.1103/PhysRevB.99.241114 for a further analysis of the two-point correlation function $\mathcal{C}_x(t)$.
[74] S. Inglis and L. Pollet, Phys. Rev. Lett. **117**, 120402 (2016).
[75] See Supplemental Material at http://link.aps.org/supplemental/10.1103/PhysRevB.99.241114 for additional data.
[76] See Supplemental Material at http://link.aps.org/supplemental/10.1103/PhysRevB.99.241114 for additional data.
[77] P. Bordia, H. Lüschen, U. Schneider, M. Knap, and I. Bloch, Nat. Phys. **13**, 460 (2017).
[78] S. Choi, J. Choi, R. Landig, G. Kucsko, H. Zhou, J. Isoya, F. Jelezko, S. Onoda, H. Sumiya, V. Khemani, C. von Keyserlingk, N. Y. Yao, E. Demler, and M. D. Lukin, Nature (London) **543**, 221 (2017).
[79] J. Zhang, P. W. Hess, A. Kyprianidis, P. Becker, A. Lee, J. Smith, G. Pagano, I. D. Potirniche, A. C. Potter, A. Vishwanath, N. Y. Yao, and C. Monroe, Nature (London) **543**, 217 (2017).
[80] L.-N Wu, A. Schnell, G. D. Tomasi, M. Heyl, and A. Eckardt, New J. Phys. **21**, 063026 (2019).
[81] R. Nandkishore, S. Gopalakrishnan, and D. A. Huse, Phys. Rev. B **90**, 064203 (2014).
[82] K. Hyatt, J. R. Garrison, A. C. Potter, and B. Bauer, Phys. Rev. B **95**, 035132 (2017).
[83] E. Levi, M. Heyl, I. Lesanovsky, and J. P. Garrahan, Phys. Rev. Lett. **116**, 237203 (2016).
[84] M. Schmitt and M. Heyl, SciPost Phys. **4**, 013 (2018).
[85] G. Carleo and M. Troyer, Science **355**, 602 (2017).
[86] S. A. Weidinger, S. Gopalakrishnan, and M. Knap, Phys. Rev. B **98**, 224205 (2018).